AIP Applied Physics Letters

Direct observation of ferroelectric polarization-modulated band bending at oxide interfaces

B. C. Huang, Y. T. Chen, Y. P. Chiu, Y. C. Huang, J. C. Yang, Y. C. Chen, and Y. H. Chu

Citation: Applied Physics Letters **100**, 122903 (2012); doi: 10.1063/1.3691615
View online: http://dx.doi.org/10.1063/1.3691615
View Table of Contents: http://scitation.aip.org/content/aip/journal/apl/100/12?ver=pdfcov
Published by the AIP Publishing

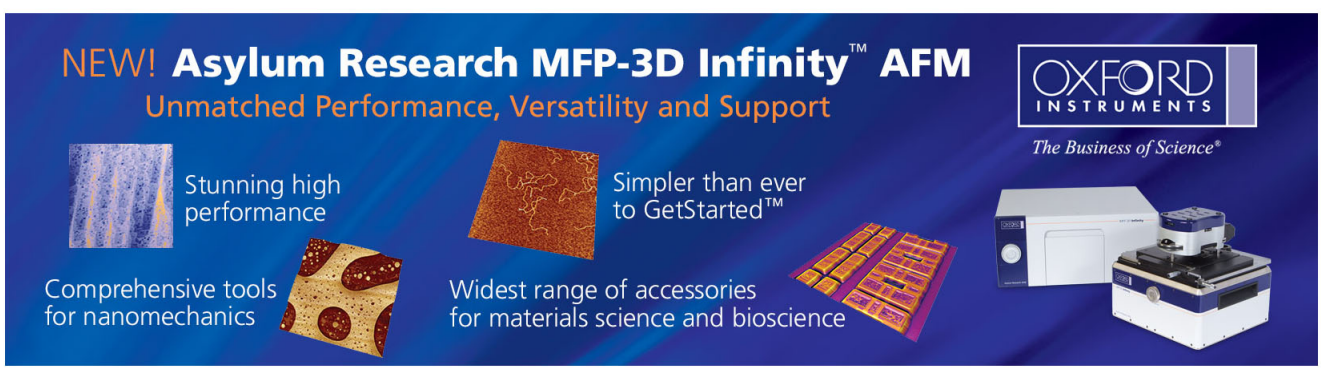

Direct observation of ferroelectric polarization-modulated band bending at oxide interfaces

B. C. Huang,[1] Y. T. Chen,[1] Y. P. Chiu,[1,a)] Y. C. Huang,[2] J. C. Yang,[3] Y. C. Chen,[2] and Y. H. Chu[3]
[1]*Department of Physics, National Sun Yat-sen University, Kaohsiung 80424, Taiwan*
[2]*Department of Physics, National Cheng Kung University, Tainan 70101, Taiwan*
[3]*Department of Materials Science and Engineering, National Chiao Tung University, Hsinchu 30010, Taiwan*

(Received 3 January 2012; accepted 12 February 2012; published online 20 March 2012)

This study presents a direct visualization of the influences of ferroelectric polarization on the electronic properties of the Schottky contact at the Nb-$SrTiO_3$/$BiFeO_3$ hetero-interface using scanning tunneling microscopy and spectroscopy (STM/S). The evolution of the local density of states across the Nb-$SrTiO_3$/$BiFeO_3$ interface reveals the interfacial band alignment and the characteristic quantities of the metal/ferroelectric contact. The unique combination of STM and STS in this study delivers an approach to obtain critical information on the interfacial electronic configurations of ferroelectric oxide interfaces and also their variation with ferroelectric polarization switching. © *2012 American Institute of Physics*. [http://dx.doi.org/10.1063/1.3691615]

Tailoring heterojunctions by manipulating the local coupling of materials in complex oxides has recently become a popular area on generating functionalities unavailable in bulk systems.[1–3] In ferroelectric heterostructures, spontaneous electrical polarization provides a particularly rich set of behaviors because of charge redistribution under the polarization effects. This has been shown to be a powerful approach to create and manipulate the degrees of freedom at the interface.[4–6] Previous studies that consider the framework of band lineups at a metal/ferroelectric heterojunction are based on the classical case of metal/semiconductor Schottky contacts with an additional input of a ferroelectric polarization.[7,8] Predictions based on the proposed model for the metal-ferroelectric interfaces can qualitatively explain current-voltage and capacitance-voltage characteristics in transport experiments.[9–11] Previous studies have experimentally investigated remarkable electronic transport properties in various ferroelectrics, revealing the interplay between electronic properties and ferroelectric polarization. Despite comprehensive theoretical and experimental surveys of the polarization-induced rectification at ferroelectric surfaces,[4,12,13] the limitations of experimental techniques have prevented *direct* and *local* measurements on an atomic scale.

This study experimentally demonstrates the direct observation of electronic structures at the metal/ferroelectric interface in a cross-sectional geometry of the heterostructures using scanning tunneling microscopy (STM).[14–16] This study reveals the atomic-scale charge reconstruction phenomena of ferroelectric interface and presents a detailed understanding of the characteristic quantities of the Schottky contact. This study also discusses the variation of the interfacial band bending for two oppositely polarized situations in ferroelectrics.

Bismuth ferrite, $BiFeO_3$ (BFO), shows a large ferroelectric polarization, a switchable diode, and photovoltaic effect in bulk single crystals.[17–19] The polarization-modulated asymmetry of the built-in potential and depletion layer of ferroelectric films generates switchable diode-like rectifying characteristics at the ferroelectric BFO surface upon reversing the polarization.[18,19] This study takes the Schottky interface between the ferroelectric BFO and the conducting Nb-doped $SrTiO_3$ (Nb-STO) as a model metal/ferroelectric system to *directly* and *locally* reveal the polarization-dependent electric structures at the metal/ferroelectric interfaces.

120-nm-thick BFO thin films were epitaxially grown by pulse laser deposition on 0.5% Nb-doped $SrTiO_3$ (001) substrates (Nb-STO). The as-grown down polarized (P-down) BFO [Fig. 1(a), left side] (i.e., with direction of polarization pointing from BFO surface to the interface of BFO/Nb-STO) was grown under 100 mTorr oxygen pressure at 700 °C. After the growth, applying an electric field, the polarization of BFO can be switched [Fig. 1(b)]. This makes it possible to change the direction of polarization pointing at the BFO/Nb-STO interface [Fig. 1(a), right side]. Thus, two oppositely polarized BFO films on Nb-STO provide a solid foundation for investigating the polarization-dependent interfacial electronic structures of the metal/ferroelectric contacts.

For STM studies, the sample was cleaved *in situ*, and measurements were performed from the cross-sectional geometry in an ultrahigh vacuum (UHV) chamber with a base pressure of $\sim 5 \times 10^{-11}$ Torr. Figure 2(a) presents a schematic illustration of the physical situation in cross-sectional STM

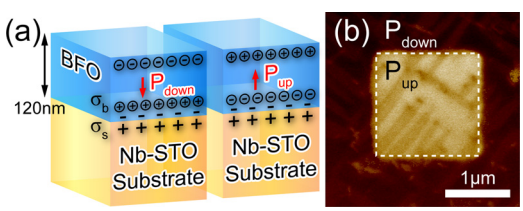

FIG. 1. (Color online) (a) Schematic illustrations of BFO/Nb-STO in the work. (Left) The as-grown downward polarized BFO/Nb-STO. (Right) The upward polarized BFO/Nb-STO after the electrically poling process. (c) Out-of-plane piezoresponse images for downward (P_{down}) and upward (P_{up}) polarized domains at the electrically poling process.

a)Author to whom correspondence should be addressed. Electronic mail: ypchiu@mail.nsysu.edu.tw.

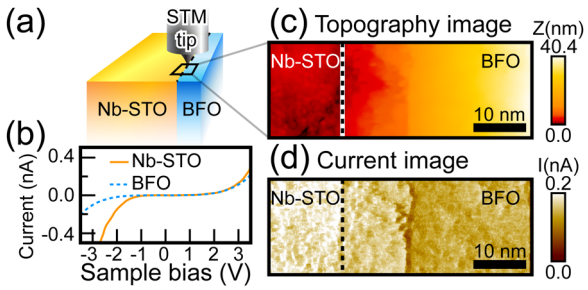

FIG. 2. (Color online) (a) Schematic XSTM measurements. (b) The spectroscopic measurements on BFO (dashed blue curve) and Nb-STO (solid orange curve) surfaces. (c) Topography and (d) the corresponding current image of BFO/Nb-STO. STM images are taken at a sample bias of +3.5 V and tunneling current of 200 pA.

(XSTM) measurements. In addition, scanning tunneling spectroscopy (STS) images were simultaneously acquired at ~100 K temperatures.

To identify the location of the interface between BFO and Nb-STO, as Fig. 2(b) shows, the epitaxial layers can be characterized with reference to the electronically specific tunneling spectra between BFO and Nb-STO. Figures 2(c) and 2(d) show a schematic cross-sectional overview of the epitaxial hetero-structure and the corresponding current images, respectively. The black dotted line in Fig. 2 indicates the position of the interface. Recording the interface makes it possible to investigate the critical electronic property at the metal/ferroelectric interface in greater detail using tunneling spectra measurements.

Figure 3 presents detailed spatially resolved spectroscopic measurements through the BFO/Nb-STO hetero-interface. The colored solid bars in the Fig. 3(a) topography image mark the spatial positions across the interface. The corresponding tunneling spectra shown in Fig. 3(b) are measured for the downward-polarized (P down), and those spectra shown in Fig. 3(c) are for upward-polarized (P up) situation in BFO films. Dotted gray colored spectra belong to the spectroscopic results of Nb-$SrTiO_3$ substrate. Solid blue colored spectra belong to the spectroscopic results of thin $BiFeO_3$ film from the position near the BFO/Nb-STO interface [the solid dark blue spectrum *i* in Fig. 3(b) and spectrum *iii* in Fig. 3(c)] to that away from the interface [the solid light blue spectrum *ii* in Fig. 3(b) and spectrum *iv* in Fig. 3(c)].

When we specifically analyze the spectrum *i* and spectrum *ii* extracted from Fig. 3(b) for the downward-polarized state in BFO, the downward band bending and the built-in potential of ~1.00 V occur on the BFO side of the interface for the downward-polarized situation in BFO film.[20,21] However, when we specifically analyze the spectrum *iii* and spectrum *iv* extracted from Fig. 3(c) for the upward polarized state in BFO, the downward band bending and the built-in potential of ~0.20 V occur on the BFO side of the interface for the upward-polarized situation in BFO film.[21] The value of the band shift is determined within the experimentally reasonable error range of the energies (~+/−0.10 eV). Based on the characteristics of the spatial spectroscopic measurements shown in Figs. 3(b) and 3(c), the evolution of band alignment across the hetero-interface can be mapped and shown in Figs. 3(f) and 3(g) in the work.

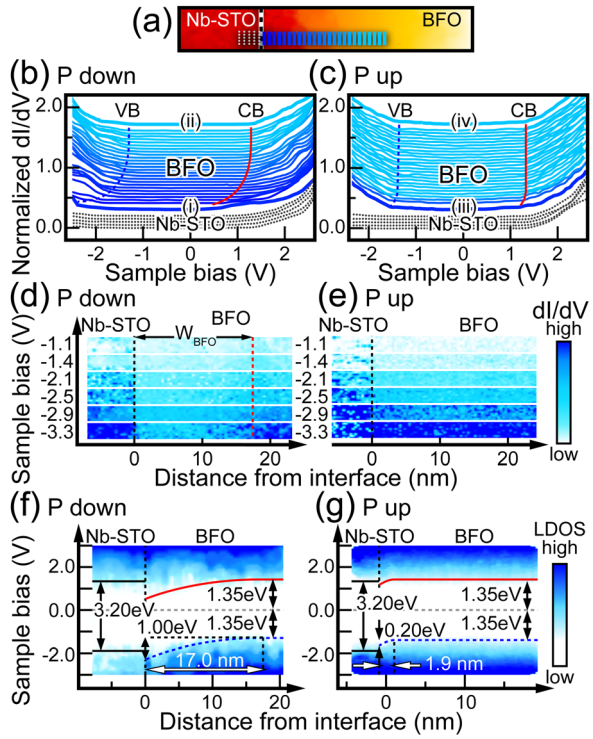

FIG. 3. (Color online) (a) Topography image of BFO/Nb-STO. *dI/dV* curves through the interface for the downward-polarized [P down, Fig. 3(b)] and upward-polarized [P up, Fig. 3(c)] situation in BFO films. *dI/dV* images for (d) the downward and (e) the upward polarized BFO sample. W_{BFO} represents the depletion length in BFO. Band alignment of (f) the downward and (g) the upward polarized BFO sample.

Electronic tunneling spectra were also examined and acquired using the current imaging tunneling spectroscopy (CITS) mode, where a series of tunnel current images was obtained at different sample bias voltages. Figures 3(d) and 3(e) display a series of *dI/dV* images by performing the CITS mode at the BFO/Nb-STO hetero-interface for P-down [Fig. 3(d)] and P-up [Fig. 3(e)] states. The *dI/dV* images in Fig. 3(d) reveal that an apparently depressed *dI/dV* result forms approximately ~17.0 nm away from the hetero-interface at the BFO side (W_{BFO}). In filled states, this decreased *dI/dV* may originate from a downward band bending of BFO, decreasing the density of states in the valence band available for tunneling at negative voltages. The downward band bending at the interface on the BFO side suggests that the space charge formed in the depletion layer of the semiconducting BFO at thermal equilibrium is negatively charged. By contrast, for the upward polarized state in BFO, an unapparent depletion layer developed (~1.9 nm), and the unclear gradually downward band bending of BFO side formed (~0.20 V) [Fig. 3(g)].[21]

Basically, STM technique is a suitable tool to resolve spatial variation of local electronic structures near the Fermi level (E_F) with high resolution. Also, Fermi level is set at the situation when the sample bias is zero. Therefore, Fermi level will be the reference level between tip and sample and also be the reference level in hetero-structures during STM measurements. However, to exactly determine the band edges, the tip-induced band bending (TIBB) effect should be taken into considerations during STM measurements.[15,22] According to the simulation results, the energetic positions of the conduction band (CB) and valence band (VB) edges of Nb-STO

without the applied sample bias (at zero sample bias) were extracted to be −0.06 V and −3.26 V, respectively.[21] In addition, the simulated energetic positions of the CB and VB edges of BFO without the applied sample bias are +1.33 V and −1.37 V. Low defects and no additional dopants concentrations of the present BFO sample contribute to the observation that the Fermi level of BFO nearly situates in the middle of the gap. A high level of doping in Nb-STO contributes to the result that Nb-STO acts as a degenerate semiconductor. With the calibration out of the tip-induced band bending effect, a schematic band alignment of the Nb-STO/BFO hetero-interface can be concisely illustrated in Fig. 4.

The ideal determination of built-in potential (ϕ_{bi}) at the metal/ferroelectric interface can be determined based on the difference of the work function between metal and semiconductor. The work function of Nb-STO is 4.08 eV and BFO is 4.70 eV [Fig. 4(a)].[9] Consequently, when Nb-STO and the as-grown P-down state in BFO are hetero-joined together, the ideal value of ϕ_{bi} is 0.62 eV. In addition, some of the electrons in Nb-STO move spontaneously into BFO because the Fermi level of BFO is lower than that of Nb-STO. This movement of electrons causes negative charges to accumulate in BFO depletion layer. Without considering the contribution of the as-grown polarization, the band structure of virgin BFO/Nb-STO can be schematically plotted in Fig. 4(b).

According to the theoretical estimation,[23] the surface charge neutrality level (ϕ_0) is located ~2.20 eV above the valence band edge. The ϕ_{bi} value of 0.62 eV, thus, suggests the Fermi level at BFO/Nb-STO interface is below ϕ_0 and results in the positively charged interface. However, to be a stable system, the as-grown interface-trap charge prefers to be zero, suggesting the Fermi level of BFO approaches to the surface charge neutrality level at the BFO/Nb-STO interface. The consideration, thus, motivates the as-grown polarization state to be downward. The positive bound charges of the as-grown P-down state in BFO will assist the reduction of the unwanted positive trapped charges at the hetero-interface. Consequently, the depolarization field resulting from the as grown polarization contributes to a wider electron region of the band at the interface, as schematically indicated in Fig. 4(c).

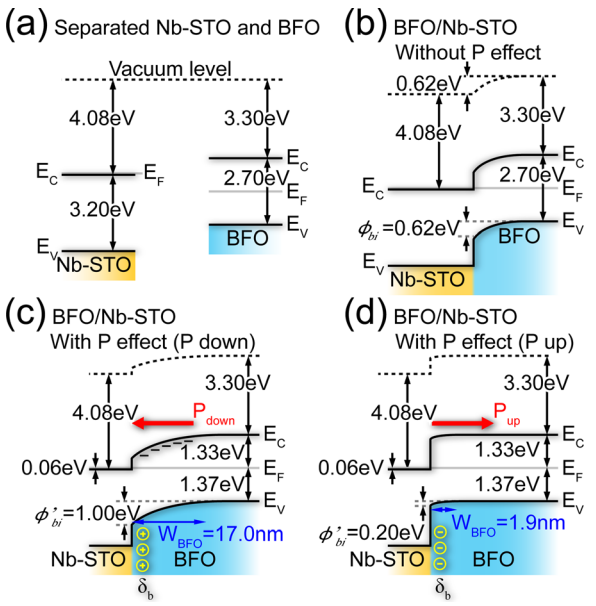

FIG. 4. (Color online) Schematic energy band diagrams for (a) separated Nb-STO and BFO; (b) Nb-STO and BFO contact in thermal equilibrium, without applied bias and without the consideration of the polarization effect; (c) the downward polarized BFO/Nb-STO; and (d) the upward polarized BFO/Nb-STO. W_{BFO} and δ_b represent the depletion length and bound charges in BFO, respectively.

According to the model proposed in Ref. 7, the influence of ferroelectric polarization on the built-in potential can introduce an additional value, $\Delta\phi = \phi'_{bi} - \phi_{bi} = \pm P\delta/\varepsilon_0\varepsilon_s$, where ϕ'_{bi} is the built-in potential with contribution from polarization, ϕ_{bi} is the built-in potential without contribution from polarization, ε_0 is the permittivity of free space, ε_s is the static dielectric constant, P is ferroelectric polarization, and δ is the thickness of an interface layer between the polarization surface charge and the physical interface with the metallic system. For BFO films, the ferroelectric polarization value P is approximately 60 $\mu C/cm^2$, and the reported low-frequency dielectric constant is approximately 100.[24] The variation in the built-in potential $\Delta\phi$ can then be estimated as the value of ~0.38 eV for a δ value of the order of a unit cell, 0.5 nm. With the considerations of ϕ_{bi} (0.62 V) and $\Delta\phi$ (0.38 V), the predicted ϕ'_{bi} (1.00 V) for a downward polarized BFO is largely consistent with the experimental observations in this study. More characteristic quantities of the contact can also be analyzed using the relations predicted in Ref. 7. In the polarized downward case, and considering the apparent built-in potential (~1.00 V) and the deletion width (~17.0 nm) shown from our measurements, the analyzed value of the effective charge density in the depleted layer N_{eff} is approximately $3.8 \times 10^{19}\,cm^{-3}$. In addition, the maximum electric field at the interface E developed at the interface is $\sim 8.0 \times 10^3$ kV/cm.

The value of the built-in potential, ϕ_{bi} (0.62 V), and the deduced value of the variation in the built-in potential, $\Delta\phi$ (0.38 V), also suggest the *ideal* built-in potential for the polarization up case is ~0.24 V. The predicted ϕ'_{bi} (0.24 V) for an upward polarized BFO is largely consistent with the experimental ϕ'_{bi} (0.20 V) in this study. As schematically shown in Fig. 4(d), the analyses figuratively explained the physically reverse situation when the P-up ferroelectric BFO film contacts the Nb-STO substrate. In this case, the depolarization field from the negative bound charges results in the upward-bending of the band and produces a narrow depletion region near the interface. A comprehensive interpretation of the related electronic properties in the P-up case explains the formation of an unapparent depletion layer and the built-in potential of P-up state in BFO. Opposite band variations demonstrate that tailoring the polarization direction in ferroelectric films can significantly alter modulated metal/ferroelectric Schottky barriers.

In conclusion, this study applies XSTM to visualize the influence of the ferroelectric polarization on the interfacial electronic properties in metal/ferroelectric hetero-junctions. The STM results in this study demonstrate a way to directly and locally investigate the polarization-modulated electronic structures in metal/ferroelectric hetero-structures.

The authors would like to thank the National Science Council of the Republic of China, Taiwan, for financially supporting this research under Contract Nos. NSC 98-2112-M-110-005-MY3 and NSC-100-2119-M-009-003.

[1]A. Ohtomo and H. Y. Hwang, Nature (London) **427**, 423 (2004).
[2]J. Chakhalian, J. W. Freeland, G. Srajer, J. Strempfer, G. Khaliullin, J. C. Cezar, T. Charlton, R. Dalgliesh, C. Bernhard, G. Cristiani, H.-U. Habermeier, and B. Keimer, Nat. Phys. **2**, 244 (2006).
[3]A. Gozar, G. Logvenov, L. Fitting Kourkoutis, A. T. Bollinger, L. A. Giannuzzi, D. A. Muller, and I. Bozovic, Nature **455**, 782 (2008).
[4]P. Maksymovych, S. Jesse, P. Yu, R. Ramesh, A. P. Baddorf, and S. V. Kalinin, Science **324**, 1421 (2009).
[5]C. L. Wu, P. W. Lee, Y. C. Chen, L. Y. Chang, C. H. Chen, C. W. Liang, P. Yu, Q. He, R. Ramesh, and Y. H. Chu, Phys. Rev. B **83**, 020103(R) (2011).
[6]L. Pintilie, C. Dragoi, and I. Pintilie, J. Appl. Phys. **110**, 044105 (2011).
[7]L. Pintilie and M. Alexe, J. Appl. Phys. **98**, 124103 (2005).
[8]L. Pintilie, I. Boerasu, M. J. M. Gomes, T. Zhao, R. Ramesh, and M. Alexe, J. Appl. Phys. **98**, 124104 (2005).
[9]H. Yang, H. M. Luo, H. Wang, I. O. Usov, N. A. Suvorova, M. Jain, D. M. Feldmann, P. C. Dowden, R. F. DePaula, and Q. X. Jia, Appl. Phys. Lett. **92**, 102113 (2008).
[10]L. Pintilie, C. Dragoi, Y. H. Chu, L. W. Martin, R. Ramesh, and M. Alexe, Appl. Phys. Lett. **94**, 232902 (2009).
[11]C. J. Won, Y. A. Park, K. D. Lee, H. Y. Ryu, and N. Hur, J. Appl. Phys. **109**, 084108 (2011).
[12]C.-H. Yang, J. Seidel, S. Y. Kim, P. B. Rossen, P. Yu, M. Gajek, Y. H. Chu, L. W. Martin, M. B. Holcomb, Q. He, P. Maksymovych, N. Balke, S. V. Kalinin, A. P. Baddorf, S. R. Basu, M. L. Scullin, and R. Ramesh, Nature Mater. **8**, 485 (2009).
[13]W. Wu, J. R. Guest, Y. Horibe, S. Park, T. Choi, S.-W. Cheong, and M. Bode, Phys. Rev. Lett. **104**, 217601 (2010).
[14]Y. P. Chiu, Y. T. Chen, B. C. Huang, M. C. Shih, J. C. Yang, Q. He, C. W. Liang, J. Seidel, Y. C. Chen, R. Ramesh, and Y. H. Chu, Adv. Mater. **23**, 1530 (2011).
[15]Y. P. Chiu, B. C. Huang, M. C. Shih, J. Y. Shen, P. Chang, C. S. Chang, M. L. Huang, M.-H. Tsai, M. Hong, and J. Kwo, Appl. Phys. Lett. **99**, 212101 (2011).
[16]Y. P. Chiu, B. C. Chen, B. C. Huang, M. C. Shih, and L. W. Tu, Appl. Phys. Lett. **96**, 082107 (2010).
[17]T. Choi, S. Lee, Y. J. Choi, V. Kiryukhin, and S.-W. Cheong, Science **324**, 63 (2009).
[18]C. Wang, K. J. Jin, Z. T. Xu, L. Wang, C. Ge, H. B. Lu, H. Z. Guo, M. He, and G. Z. Yang, Appl. Phys. Lett. **98**, 192901 (2011).
[19]C. Ge, K. J. Jin, C. Wang, H. B. Lu, C. Wang, and G. Z. Yang, Appl. Phys. Lett. **99**, 063509 (2011).
[20]R. M. Feenstra, Phys. Rev. B **50**, 4561 (1994).
[21]See supplementary material at http://dx.doi.org/10.1063/1.3691615 for the determination of the energy shift of $BiFeO_3$ side for the downward/upward polarized state in $BiFeO_3$ and the determination of the energy band edges of $BiFeO_3$ and Nb-$SrTiO_3$.
[22]N. Ishida, K. Sueoka, and R. M. Feenstra, Phys. Rev. B **80**, 075320 (2009).
[23]S. J. Clark and J. Robertson, Appl. Phys. Lett. **90**, 132903 (2007).
[24]J. Li, J. Wang, M. Wuttig, R. Ramesh, N. Wang, B. Ruette, A. P. Pyatakov, A. K. Zvezdin, and D. Viehland, Appl. Phys. Lett. **84**, 5261 (2004).